

AttDLNet: Attention-based DL Network for 3D LiDAR Place Recognition

Tiago Barros, Luís Garrote, Ricardo Pereira, Cristiano Premebida, Urbano J. Nunes

Abstract—Deep networks have been progressively adapted to new sensor modalities, namely to 3D LiDAR, which led to unprecedented achievements in autonomous vehicle-related applications such as place recognition. One of the main challenges of deep models in place recognition is to extract efficient and descriptive feature representations that relate places based on their similarity. To address the problem of place recognition using LiDAR data, this paper proposes a novel 3D LiDAR-based deep learning network (named AttDLNet) that comprises an encoder network and exploits an attention mechanism to selectively focus on long-range context and inter-feature relationships. The proposed network is trained and validated on the KITTI dataset, using the cosine loss for training and a retrieval-based place recognition pipeline for validation. Additionally, an ablation study is presented to assess the best network configuration. Results show that the encoder network features are already very descriptive, but adding attention to the network further improves performance. From the ablation study, results indicate that the middle encoder layers have the highest mean performance, while deeper layers are more robust to orientation change. The code is publicly available on the project website: <https://github.com/Cybonic/AttDLNet>

I. INTRODUCTION

Place recognition has been the focus of much research over the last decade with particular interest by the autonomous vehicle community, which uses place recognition to achieve long-term localization. Place recognition is a perception-based approach that recognizes previously visited places using visual, structural, and/or semantic cues. Although multiple approaches [1], [2] have been proposed for place recognition with promising results in appearance changing and extreme viewpoint variation scenarios, some fundamental problems are still open for research: perceptual aliasing (*i.e.*, places with similar appearance generated from two distinct locations); observations taken over time in the same location that exhibit significant appearance changes due to day-night variation weather, seasonal or structural changes; and viewpoint invariance.

Although vision-based approaches have been the most used methods, structural-based approaches are gaining more popularity lately. In particular, research has been focusing on approaches that rely on 3D LiDAR sensors, which capture 360° of their surroundings. The structural information returned by these sensors has proven to be descriptive enough for place recognition (as illustrated in Fig. 1) and additionally to be robust to appearance change, which is an advantage

The authors are with the University of Coimbra, Institute of Systems and Robotics, Department of Electrical and Computer Engineering, Portugal. E-mails: {tiagobarros, garrote, ricardo.pereira, cpremebida, urbano}@isr.uc.pt

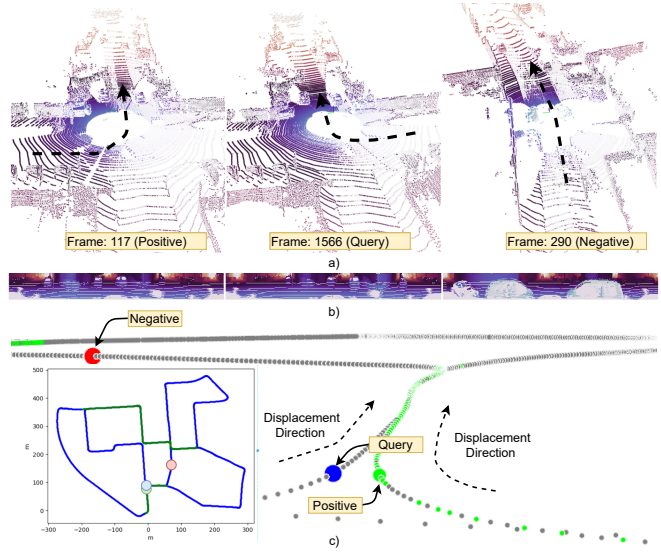


Fig. 1. Illustration of a query, a positive and a negative frame of sequence 00 - extracted from the KITTI dataset. The above representations correspond to: a) point clouds, b) spherical-based range (proxy) model input, c) geometrical localization.

compared to vision approaches. An additional factor that popularized LiDAR sensors in place recognition is the recent improvements in deep learning (DL), namely the capability to learn a given task on point clouds in an end-to-end fashion.

In place recognition, the research of 3D deep learning approaches has been focused on learning robust, discriminative, and generalizable descriptors from point clouds, which remains an open problem. A very common approach to generate such global descriptors from point clouds is to use methods such as VLAD (Vector of Locally Aggregated Descriptors), which aggregate local features into global descriptors [3]. Another research direction is to formulate the place recognition problem as a graph matching problem, using for example point cloud segmentation approaches [4]. These approaches consider each feature equally, disregarding relationships between features or contextual information. A solution to this problem, cf. the approach presented in this work, is to use attention mechanisms, which exploit feature relationships using attention maps.

This work proposes, for point cloud-based place recognition, a novel deep learning network for descriptive descriptor generation. The proposed **Attention-based Deep Learning Network**, hereafter called AttDLNet, takes advantage of RangeNet++'s [5] backbone architecture (a state-of-the-art point cloud segmentation approach) for feature extraction

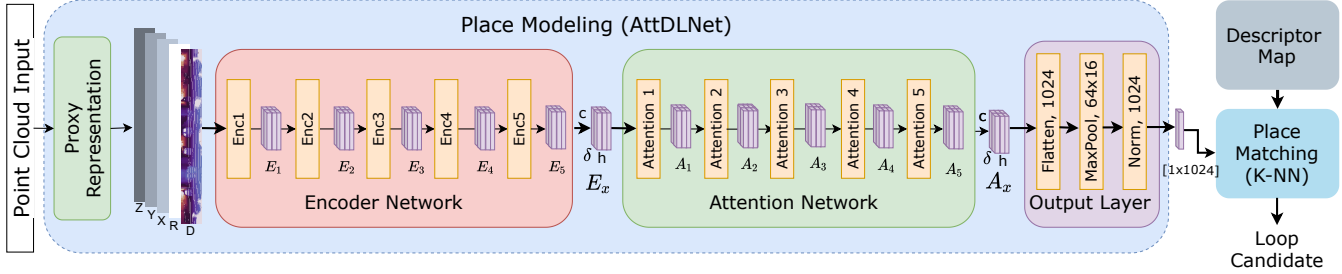


Fig. 2. Proposed place recognition pipeline with three key modules: place modeling, place matching, and descriptor map. The map contains all descriptors, which are loaded offline. Place matching is computed using a K-nearest neighbor approach that employs cosine similarity for descriptor comparison. Place modeling is computed using AttDLNet: an attention-based network for 3D LiDAR data. AttDLNet receives a point cloud as input; converts the point cloud to a proxy representation, which is a spherical-based range representation; extracts features from the proxy representation using the encoder network; then calculates relationships among features using an attention network; and finally a descriptor is outputted by output layer, which employs max-pooling and flatten

(described in Section IV), which outputs highly efficient and descriptive point-cloud features from a range-based proxy representation. Figure 1 illustrates points clouds and the corresponding range-based representation used in this work. Additionally, an attention network is used to learn long-range context and inter-feature relationships. Succinctly, the main contributions of this work are:

- an attention-based DL network (see Fig. 2) for the task of 3D LiDAR-based place recognition, which leverages an attention network to learn long-range relationships;
- an extensive ablation study of the AttDLNet while performing place recognition to obtain an optimal architecture.

II. RELATED WORK

Over the last few years, place recognition has been the subject of much research using DL approaches. Place recognition benefited immensely from the recent developments both in supervised and unsupervised learning, which have been widely applied to vision [6], structural [7] or both modalities combined [8]. The structural modality, in particular, has gained more attention with the recent DL architectures, which learn features in an end-to-end manner from point clouds.

In point cloud-based DL approaches, the networks can be split into two main categories based on the input representation: networks that learn directly from point clouds [3], [9], or networks that learn indirectly from point clouds, learning from proxy representations instead. Proxy representations are mainly structured-grid representations such as voxels [10], depth range images [7], which are naturally handled by 2D CNNs [7] or 3D CNNs [11] for feature learning. Point clouds, on the other hand, are irregular and unstructured, which makes feature learning, using traditional DL approaches, challenging. In place recognition, place descriptors are learned directly from point clouds using PointNetVLAD [3]. PointNetVLAD employs a symmetric max pooling function to aggregate local point features to make the output permutation invariant, which is crucial for place description. Another approach to map raw point clouds directly to descriptors is proposed in [12], where a

graph-based neighborhood aggregation approach is used to extract local structures and reveal the spatial distribution of local features. A graph-based approach is also proposed in [4], which models place recognition as a graph matching problem, using as input segmented point clouds.

More recently, various segmentation, retrieval, and place recognition works have been exploiting spatial and contextual relationships from features using attention mechanisms. In [13], a Local Attention-Edge Convolution layer is proposed for the task of segmentation, which leverages local graphs of neighborhood points searched in multi-directions. Attention is used locally on the graph edges and used globally to learn long-range spatial contextual features. A graph approach is also proposed in [14] for the same task, proposing a graph attention convolution where the kernels assume dynamic shapes to adapt to an object's structure. Regarding place recognition, attention is used by PCAN [15] during the feature aggregation process of local features, which are extracted by an approach inspired on PointNet [16]. The attention is employed in the NetVLAD [17] layer as a context-aware reweighting network to learn multi-scale textual information. A similar approach is proposed in SOE-Net [18], but the local features are modeled based on a point orientation encoder. Contrary to the single modality works aforementioned, PIC-Net [19] uses attention to combine image and point cloud features.

III. PROPOSED APPROACH

The place recognition approach presented here is formulated as a retrieval task, as illustrated in Fig. 2. The pipeline comprises three basic modules: place modeling, place matching, and descriptor map. The descriptor map is dedicated to maintaining all descriptors, while the place matching module is responsible for returning loop candidates using a k-nearest neighbor (K-NN) approach, which employs a cosine similarity distance for descriptor comparison. These descriptors are generated in the place modeling module, which maps point clouds to a descriptive feature space using the AttDLNet.

AttDLNet is a deep-learning network that performs the following: converts point clouds to a range-based proxy rep-

resentation; extracts features from the representation using a encoder network; computes feature relationships using an attention network; converts the features maps to adequate descriptors in the output layer.

A. Proxy Representation

The proxy representation used in this work is a spherical-based range representation inspired by the work in [5]. A point $p_i = (x, y, z)$, belonging to a point cloud P with a range value of r , is projected to spherical coordinate system and then to a image space (u, v) given by:

$$\begin{pmatrix} u \\ v \end{pmatrix} = \begin{pmatrix} \frac{1}{2}[1 - \arctan(x, y)\pi^{-1}] \omega \\ [1 - (\arcsin(zr^{-1}) + f_{up})f^{-1}] h \end{pmatrix} \quad (1)$$

where (u, v) corresponds to the pixel coordinates, (w, h) are the width and height of the output image tensor, $f = f_{up} + f_{down}$ and f_{up} are the sensor's total and upper vertical field-of-view, respectively.

Thus, a point cloud is projected to a grid-based representation with a vertical resolution h , rotational resolution ω , and 5 channels (i.e., D, R, X, Y, Z). Additionally, to range values (D), the input representation has a channel for each (x, y, z) coordinates (X, Y, and Z), and a channel for remission measurements (R) (i.e., measurements of diffuse reflection). The final tensor with shape $[5 \times h \times \omega]$ is fed to the encoder network for feature learning.

B. Encoder Network

The encoder network has the aim of learning features from a range-based proxy representation. The network used in this work is an adapted version of DarkNet53 [20], which was originally proposed for image-based object detection [20] and more recently adapted for point cloud-based segmentation in [4], demonstrating in both tasks high levels of descriptiveness. The network comprises several stacked encoder layers (e.g., 2D Convolution, BatchNormalization, and LeakyReLU) with skip connections, receiving as input a tensor with shape $[5 \times h \times \omega]$. The encoder network proposed in [4], which is adopted for this work, has five encoder layer (has illustrated in Fig.2); each encoder layer downsamples previous layer's tensor in the horizontal (rotational) direction, while the vertical shape is kept. The network's performance is studied in Section IV-D, where an ablation study is conducted to asses the best architecture for place recognition. The network configuration that returns the best performance will be used as final encoder network, which may differ from the architecture presented in Fig.2.

C. Attention Network

Inspired by the work presented in [21], where an attention mechanism is used to learn image features, this work proposes a similar approach to learn point cloud features but, instead of only one layer, this work proposes a network of attention layers (AN).

The proposed attention network (AN) comprises four attention layers (AL). The network was limited to four due to

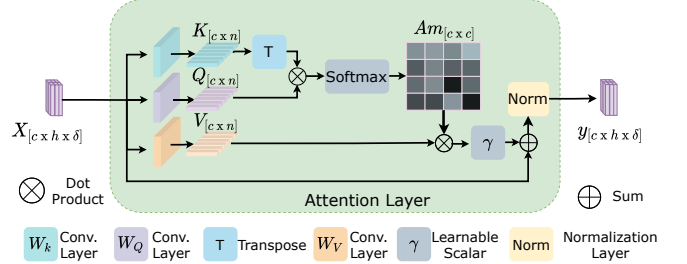


Fig. 3. Attention layer with \mathbf{X} and \mathbf{Y} being the input and output, respectively with the same dimension.

computational constraints. Each AL represents a dot-product attention mechanism as shown in Fig.3, which comparatively with additive attention [22] is much faster and more space-efficient due to being computationally implementable through highly optimized matrix multiplication code [23].

The AL has an input (X) with shape $[c \times h \times \delta]$ and an output (Y) with the same shape. The input is mapped into new features spaces $K = W_K x$, $Q = W_Q x$ and $V = W_V x$ with K , Q and V with shape $[c \times n]$, where $n = h \times \delta$. The matrices W_K , W_Q and W_V are learned during training using convolutional layers. Furthermore, K and Q are used to compute the attention map $A_m \in \mathbb{R}^{c \times c}$ (2), which improves the feature representation capabilities [13]:

$$A_m = \frac{e^{Q^T K}}{\sum_{n=1}^n e^{Q^T K}} \quad (2)$$

Finally, the output is computed using (3), where γ is a trainable scalar,

$$y = x + \gamma A_m V. \quad (3)$$

D. Output Layer

The output comprises three main operations. Firstly, max pooling is applied to the input, converting the tensor from shape $[c \times h \times \delta]$ to $[h \times \delta]$. Secondly, the tensor is flatten assuming the final shape $[1 \times m]$, where $m = h \times \delta$. Finally, the flattened tensor is normalized using layer normalization.

IV. EXPERIMENTS AND RESULTS

An experimental evaluation was conducted to support AttDLNet's suitability for place recognition. Moreover, an ablation study is used to select the best network architecture. All the experiments in this work have been carried out on the KITTI odometry dataset, using only the sequences that comprise segments with loops.

A. KITTI Odometry Benchmark

The KITTI Odometry Benchmark [24] is a collection of 22 sequences, containing point clouds, images, and GPS recordings of inner-city traffic, residential areas, highway scenes, and countryside roads around Karlsruhe, Germany. The sequences are split in training set (sequences 00 to 10) and test set (sequences 11 to 21). The point clouds are recorded by a Velodyne 64 HDL sensor at 10 Hz, placed on the center of the car's roof. Ground truth poses are provided by an RTK GPS sensor.

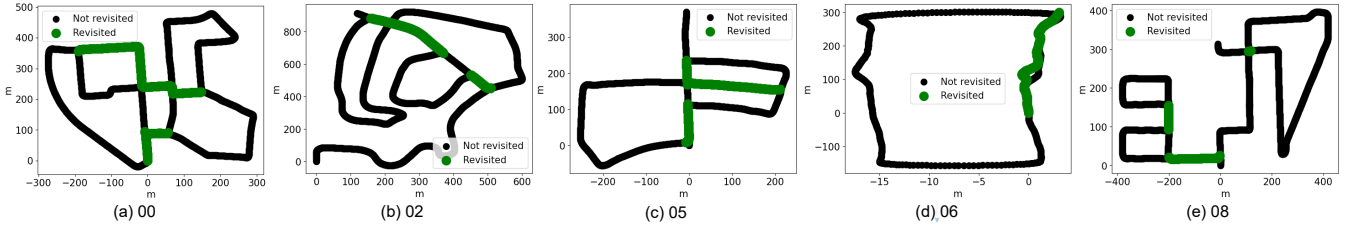


Fig. 4. KITTI Odometry Benchmark sequences used in this work, with the loop segments (in green) and segments with no loops (in black) highlighted: a) 00, b) 02, c) 05, d) 06 and e) 08. Sequences 00, 02, 05 and 06 contain segments that are always revisited from the same direction, while sequence 08 contains segments that are revisited from opposing direction. For example, in (a) black segments represent locations that were not revisited, while green segments represent locations that were revisited.

However, not all sequences contain loops. Only the sequences 00, 02, 05, 06, and 08 have substantial segments with revisited paths, which were used in this work to train and validate the proposed approach. Figure 4 illustrates all sequences and respective loop segments (in green) and segments with no loops (in black). Moreover, sequences 00, 02, 05, 06 have loop segments that are revisited from the same direction; while sequence 08 has loop segments that are only revisited from the opposite direction, which is particularly useful to validate viewpoint invariance.

B. Ground-truth Data and Evaluation

The ground truth data was generated based on a loop criteria where two point clouds form a loop (*i.e.*, $c_q = 1$, where c is the loop class) whenever a query (P_q) - frames belonging to a revisited segment in the map - and its nearest neighbor P_{nn} are within a radius of r_{th} in the map (*i.e.*, $\|P_q - P_{nn}\|_2 \leq r_{th}$), otherwise no loop exists and $c_q = 0$. For this work r_{th} is set to 6 m *i.e.*, a loop exists whenever frames from different revisits are within a range of 6m. Table I contains the frames length and the number of loops detected in each sequence. The ground truth loops are illustrated in Fig. 4.

The evaluation is performed using 5-fold cross-validation, where each fold represents a sequence. For example, to validate the network on sequence 00, the network is trained on the remaining 4 sequences. The evaluation metric used to measure AttDLNet's performance is F1, which is computed through precision (Eq. 4) and recall (Eq. 5). In retrieval-based place recognition tasks, precision measures the fraction of correct retrieved loop frames among all retrieved frames, while recall measures the fraction of correct retrieved loop frames within all loops. Table II shows the confusion matrix used for retrieval-based place recognition, where the true positives are retrieved frames that are real loops; false negatives are retrieved frames that are not loops; true negatives are frames that are not retrieved and that are not loops; and false negatives are frames that are not retrieved but are loops (*i.e.*, missed loops).

$$\text{Precision} = \frac{\text{TP} (\# \text{ Retrieved Loops})}{\text{TP} + \text{FP} (\# \text{ Retrieved Frames})} \quad (4)$$

$$\text{Recall} = \frac{\text{TP} (\# \text{ Retrieved Loops})}{\text{TP} + \text{FN} (\# \text{ Loops})} \quad (5)$$

TABLE I
DATASET AND LOOP INFORMATION.

Sequence:	00	02	05	06	08
Length [frames]:	4051	4661	2761	1101	4071
Loops [frames]:	801	306	489	265	329

TABLE II
CONFUSION MATRIX TO EVALUATE RETRIEVAL-BASED PLACE
RECOGNITION

	Loops	Not Loops
Retrieved	True Positives (TP)	False Positives (FP)
Not Retrieved	False Negatives (FN)	True Negatives (TN)

C. Implementation and Training Setup

The AttDLNet was implemented on PyTorch [25] and run on a hardware setup with an NVIDIA GFORCE GTx1070Ti GPU and an AMD Ryzen 5 CPU with 32 GB of RAM. The hyperparameters are trained using the Adam optimizer [26] with a learning rate of 0.001 and the cosine embedding loss function from the PyTorch framework.

The training data is formed by the ground-truth loops (*i.e.*, a query and positive frame) and negative frames, which means that a negative frame is associated to each loop. The negative frame is a randomly selected frame that is at least 20 m apart from the query and neither belongs to the query or positive frames (as illustrated in Fig. 1).

Since place matching is computed in the cosine space, AttDLNet is trained in the same similarity space, using the cosine loss function, with a margin parameter that has to be set. To assess the best margin value, a margin study was conducted, for which AttDLNet was trained and evaluated several times, using each time a different margin value. The discrete margin values used in the study are: 0.0, 0.3, 0.5, 0.7, 0.8, 0.85, 0.9, 0.95. Training and evaluation were performed using the conditions described in previous sections.

The best margin value was 0.85, which was obtained by computing the mean F1 value of AttDLNet's retrieval performance on sequences 00, 02, 05, 06, and 08. The mean F1 curve is shown in Fig. 5.a.

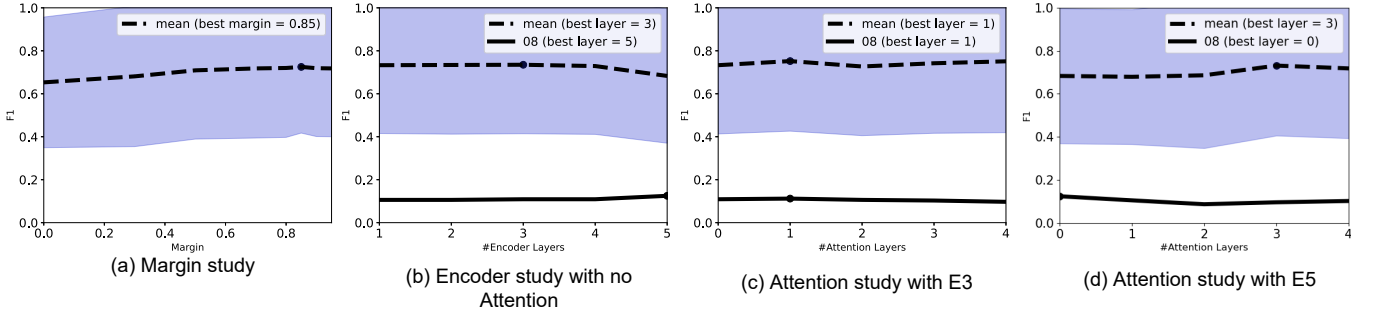


Fig. 5. AttDLNet ablation studies which include a) margin, b) encoder with no attention, c) attention with E3 encoder configuration, and d) attention with E5 encoder configuration.

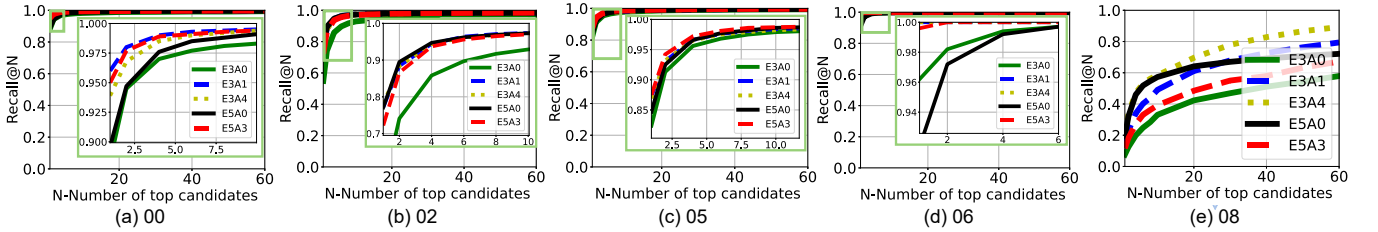


Fig. 6. Recall scores of E3A0, E3A1, E3A4, E5A0 and E5A3 AttDLNet's architectures on sequence: a) 00, b) 02, c) 05, d) 06 and e) 08.

TABLE III

F1 SCORES OF THE ATTDLNET'S ENCODER AND ATTENTION ABLATION STUDY. THE ATTENTION STUDY USES THE ENCODER ARCHITECTURE THAT HAS THE HIGHEST MEAN F1, WHICH ARE E3 AND E5.

Seq.	00	02	05	06	08	mean	FPS
E1	0.90	0.82	0.86	0.98	0.11	0.73	368
E2	0.93	0.78	0.86	1.00	0.11	0.73	260
E3	0.92	0.78	0.87	1.00	0.11	0.74	103
E4	0.94	0.79	0.82	0.98	0.11	0.73	52
E5	0.94	0.55	0.85	0.95	0.13	0.68	42
E3A0	0.92	0.77	0.87	1.00	0.11	0.73	103
E3A1	0.95	0.82	0.88	1.00	0.11	0.75	78
E3A2	0.94	0.74	0.87	0.99	0.11	0.72	63
E3A3	0.94	0.80	0.88	0.99	0.10	0.74	53
E3A4	0.94	0.82	0.90	1.00	0.10	0.75	50
E5A0	0.94	0.55	0.85	0.95	0.13	0.68	42
E5A1	0.91	0.62	0.77	0.99	0.11	0.68	78
E5A2	0.94	0.54	0.89	0.98	0.09	0.69	63
E5A3	0.94	0.79	0.85	0.98	0.10	0.73	53
E5A4	0.95	0.69	0.86	0.99	0.10	0.72	50

D. Ablation Study

The study is divided in two phases. In the first phase, the study focuses on the encoder network with no attention in the pipeline; while the second phase uses the best encoder network architecture to study the attention network. Specifically, the study consists in exploiting the contribution of each layer to the overall performance, to obtain the best architecture. AttDLNet's architectures used in this study are identified by $ExAy$, where $x \in [1, 2, 3, 4, 5]$ represents the possible encoder configurations, while $y \in [0, 1, 2, 3, 4]$ represents the possible attention network configurations. For example,

$E3A1$ is a network that has three encoder layers and one attention layer *i.e.*, the output of the third encoder layer (E3) is fed directly to the attention network, which outputs A_1 to the output layer (see Fig. 2). Another example is $E3A0$, which represents AttDLNet with an encoder network having three layers and no attention. AttDLNet's output is then matched in the place matching module, using as loop prediction criteria the first nearest neighbor. Each network configuration is trained and validated in the same settings that are described in Section IV-B and IV-C.

The results of these studies are presented in Table III, where loop predictions have been considered as the first nearest neighbors, and the mean values are presented in Fig. 5 (b), (c) and (d). The results from the encoder study indicate that middle encoder layers have in general higher performance; being $E3$ the encoder configuration with the best mean performance, while $E5$ is the best network configuration on sequence 08 (which has only loops with revisits from opposing direction). Both encoder network configurations are used to perform the attention study obtaining results that have shown: by using the $E3$ configuration the best performance is obtained by A_1 and A_4 ; using the $E5$ configuration the best attention configuration is obtained by A_3 , which is lower than the $E3A1$ and $E3A4$. Moreover, the best performance on sequence 08 is obtained by $E5A0$ which means that, in terms of rotation invariance, deeper configurations with no attention are more robust, while in the other scenarios, attention improves in overall performance.

All three aforementioned AttDLNet configurations (*i.e.*, $E3A1$, $E3A4$, and $E5A3$), as well as the configurations without attention ($E3A0$ and $E5A0$), are further compared and studied in terms of retrieval performance.

E. Retrieval Performance

In this section, a retrieval performance study is presented where the number of top candidates is progressively increased in order to evaluate AttDLNet's capacity to map frames originate from the same physical space close in the feature space. It is expected that as the number of top candidates grows, more true loops are retrieved. To evaluate the network's performance, the recall metric is used, which measures the fraction of correctly retrieved loops among all loops.

To perform this study, the network architectures that have the highest performance in the ablation study were selected, which correspond to the configurations *E3A0*, *E3A1*, *E3A4*, *E5A0*, and *E5A3*; while the *N* top candidate set include $N \in [1, 2, 4, 6, 8, 10, 20, 30, 40, 50, 60]$.

The results of these studies are shown in Fig.6, indicating that network configurations with attention have in general higher performance. When analyzing results from sequence 08, where the ablation studies show that *E5A0* has the highest performance, these show that, as *N* grows, networks with attention outperform networks with no attention. This demonstrates that despite ablation studies indicating (for $N=1$) that deeper networks are more ration invariant, when *N* grows, networks with attention have a steeper performance grows, outperforming with *N* greater than 20 networks with no attention. Thus, the results indicate that attention improves place recognition in general and in particular when the number of retrieval candidates grows.

V. CONCLUSIONS

In this work, a retrieval-based place recognition architecture is proposed, which includes the novel AttDLNet network. AttDLNet is a point cloud-based DL network, which resorts to an encoder and an attention network to improve descriptiveness. The network is based on RangeNet++ which converts point clouds to range-based proxy representation. The AttDLNet can extract a feature vector from an input 3D point cloud and concurrently exploit an attention mechanism to selectively focus on the most relevant features.

The experimental evaluation (carried out on the KITTI dataset) shows that middle encoder layers have higher mean performance than early or deeper layers. However, in the particular case when places are revisited from the opposite direction, deeper layers have higher performance, i.e., more orientation invariant. When considering the place recognition pipeline, results show that the use of the AttDLNet network allows to achieve high place recognition performance.

ACKNOWLEDGMENTS

This work has been supported by the projects MATIS-CENTRO-01-0145-FEDER-000014 and SafeForest CENTRO-01-0247-FEDER-045931, Portugal. It was also partially supported by FCT through grant UIDB/00048/2020.

REFERENCES

- [1] N. Sünderhauf, S. Shirazi, F. Dayoub, B. Upcroft, and M. Milford, “On the performance of convnet features for place recognition,” in *2015 IEEE/RSJ International Conference on Intelligent Robots and Systems (IROS)*. IEEE, 2015, pp. 4297–4304.
- [2] T. Naseer, G. L. Oliveira, T. Brox, and W. Burgard, “Semantics-aware visual localization under challenging perceptual conditions,” in *2017 IEEE International Conference on Robotics and Automation (ICRA)*. IEEE, 2017, pp. 2614–2620.
- [3] M. Angelina Uy and G. Hee Lee, “Pointnetvlad: Deep point cloud based retrieval for large-scale place recognition,” in *Proceedings of the IEEE Conference on Computer Vision and Pattern Recognition*, 2018, pp. 4470–4479.
- [4] X. Kong, X. Yang, G. Zhai, X. Zhao, X. Zeng, M. Wang, Y. Liu, W. Li, and F. Wen, “Semantic graph based place recognition for 3d point clouds,” in *2020 IEEE/RSJ International Conference on Intelligent Robots and Systems (IROS)*, 2020, pp. 8216–8223.
- [5] A. Milioto, I. Vizzo, J. Behley, and C. Stachniss, “Rangenet++: Fast and accurate lidar semantic segmentation,” in *2019 IEEE/RSJ International Conference on Intelligent Robots and Systems (IROS)*. IEEE, 2019, pp. 4213–4220.
- [6] L. Wu and Y. Wu, “Deep supervised hashing with similar hierarchy for place recognition,” in *IROS*, 2019, pp. 3781–3786.
- [7] L. Schaupp, M. Bürki, R. Dubé, R. Siegwart, and C. Cadena, “OREOS: Oriented recognition of 3d point clouds in outdoor scenarios,” in *2019 IEEE/RSJ International Conference on Intelligent Robots and Systems (IROS)*, 2019, pp. 3255–3261.
- [8] A. Oertel, T. Cieslewski, and D. Scaramuzza, “Augmenting visual place recognition with structural cues,” *arXiv preprint arXiv:2003.00278*, 2020.
- [9] C. Suo, Z. Liu, L. Mo, and Y. Liu, “LPD-AE: Latent space representation of large-scale 3D point cloud,” *IEEE Access*, vol. 8, pp. 108 402–108 417, 2020.
- [10] M. Y. Chang, S. Yeon, S. Ryu, and D. Lee, “SpoxelNet: Spherical voxel-based deep place recognition for 3D point clouds of crowded indoor spaces,” in *Intelligent Robots and Systems (IROS)*, 2020, pp. 8564–8570.
- [11] R. Dubé, A. Cramariuc, D. Dugas, J. Nieto, R. Siegwart, and C. Cadena, “SegMap: 3d segment mapping using data-driven descriptors,” in *Robotics: Science and Systems (RSS)*, 2018.
- [12] Z. Liu, S. Zhou, C. Suo, P. Yin, W. Chen, H. Wang, H. Li, and Y.-H. Liu, “LPD-Net: 3D point cloud learning for large-scale place recognition and environment analysis,” in *Proceedings of the IEEE/CVF International Conference on Computer Vision*, 2019, pp. 2831–2840.
- [13] M. Feng, L. Zhang, X. Lin, S. Z. Gilani, and A. Mian, “Point attention network for semantic segmentation of 3d point clouds,” *Pattern Recognition*, vol. 107, p. 107446, 2020.
- [14] L. Wang, Y. Huang, Y. Hou, S. Zhang, and J. Shan, “Graph attention convolution for point cloud semantic segmentation,” in *Proceedings of the IEEE/CVF Conference on Computer Vision and Pattern Recognition*, 2019, pp. 10 296–10 305.
- [15] W. Zhang and C. Xiao, “PCAN: 3D attention map learning using contextual information for point cloud based retrieval,” in *Proceedings of the IEEE/CVF Conference on Computer Vision and Pattern Recognition*, 2019, pp. 12 436–12 445.
- [16] C. R. Qi, H. Su, K. Mo, and L. J. Guibas, “Pointnet: Deep learning on point sets for 3d classification and segmentation,” in *Proceedings of the IEEE conference on computer vision and pattern recognition*, 2017, pp. 652–660.
- [17] R. Arandjelovic, P. Gronat, A. Torii, T. Pajdla, and J. Sivic, “Netvlad: Cnn architecture for weakly supervised place recognition,” in *Proceedings of the IEEE conference on computer vision and pattern recognition*, 2016, pp. 5297–5307.
- [18] Y. Xia, Y. Xu, S. Li, R. Wang, J. Du, D. Cremers, and U. Stilla, “SOENet: A Self-Attention and Orientation Encoding Network for Point Cloud based Place Recognition,” *arXiv preprint arXiv:2011.12430*, 2020.
- [19] Y. Lu, F. Yang, F. Chen, and D. Xie, “PIC-Net: Point Cloud and Image Collaboration Network for Large-Scale Place Recognition,” *arXiv preprint arXiv:2008.00658*, 2020.
- [20] A. Farhadi and J. Redmon, “Yolov3: An incremental improvement,” *Computer Vision and Pattern Recognition, cite as*, 2018.
- [21] H. Zhang, I. Goodfellow, D. Metaxas, and A. Odena, “Self-attention generative adversarial networks,” in *International conference on machine learning*. PMLR, 2019, pp. 7354–7363.

- [22] D. Bahdanau, K. Cho, and Y. Bengio, “Neural machine translation by jointly learning to align and translate,” *arXiv preprint arXiv:1409.0473*, 2014.
- [23] A. Vaswani, N. Shazeer, N. Parmar, J. Uszkoreit, L. Jones, A. N. Gomez, L. u. Kaiser, and I. Polosukhin, “Attention is all you need,” in *Advances in Neural Information Processing Systems*, vol. 30, 2017.
- [24] A. Geiger, P. Lenz, and R. Urtasun, “Are we ready for autonomous driving? the KITTI vision benchmark suite,” in *Conference on Computer Vision and Pattern Recognition (CVPR)*, 2012.
- [25] A. Paszke, S. Gross, F. Massa, A. Lerer, J. Bradbury, G. Chanan, T. Killeen, Z. Lin, N. Gimelshein, L. Antiga, A. Desmaison, A. Kopf, E. Yang, Z. DeVito, M. Raison, A. Tejani, S. Chilamkurthy, B. Steiner, L. Fang, J. Bai, and S. Chintala, “Pytorch: An imperative style, high-performance deep learning library,” in *Advances in Neural Information Processing Systems*, vol. 32, 2019.
- [26] D. P. Kingma and J. Ba, “Adam: A method for stochastic optimization,” *arXiv preprint arXiv:1412.6980*, 2014.